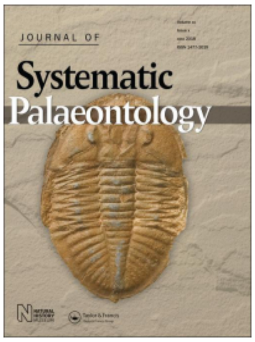

Taylor & Francis
Taylor & Francis Group

Journal of Systematic Palaeontology

ISSN: (Print) (Online) Journal homepage: https://www.tandfonline.com/loi/tjsp20

A new elasmothere genus and species from the middle Miocene of Tongxin, Ningxia, China, and its phylogenetic relationship

Danhui Sun, Tao Deng, Xiaokang Lu & Shiqi Wang

To cite this article: Danhui Sun, Tao Deng, Xiaokang Lu & Shiqi Wang (2023) A new elasmothere genus and species from the middle Miocene of Tongxin, Ningxia, China, and its phylogenetic relationship, Journal of Systematic Palaeontology, 21:1, 2236619, DOI: 10.1080/14772019.2023.2236619

To link to this article: https://doi.org/10.1080/14772019.2023.2236619

Journal of Systematic Palaeontology, 2023
Vol. 21, No. 1, 2236619
http://dx.doi.org/10.1080/14772019.2023.2236619

A new elasmothere genus and species from the middle Miocene of Tongxin, Ningxia, China, and its phylogenetic relationship

Danhui Sun[a,b], Tao Deng[a,b]*, Xiaokang Lu[c] and Shiqi Wang[b]

[a]*Department of Archaeology and Anthropology, University of Chinese Academy of Sciences, Beijing 100049, PR China;* [b]*Key Laboratory of Vertebrate Evolution and Human Origins of Chinese Academy of Sciences, Institute of Vertebrate Paleontology and Paleoanthropology, Chinese Academy of Sciences, Beijing 100044, PR China;* [c]*Department of Human Anatomy, Henan University of Chinese Medicine, Zhengzhou 450008, PR China*

(Received 4 September 2022; accepted 12 June 2023)

The elasmotheres were well diversified and widespread throughout the Neogene in Eurasia and East Africa. Here we report a new elasmothere genus and species, *Tongxinotherium latirhinum* gen. et sp. nov., from the Zhang'enbao Formation (middle Miocene) of Tongxin, Ningxia, China. The new genus is characterized by a broad and thick nasal bone, the 'U'-shaped nasal notch located at the level of P3, the anterior margin of the orbit situated at the level of M2, subhypsodont teeth covered and filled by plentiful cement, slightly developed enamel foldings, expanded protocone with anterior and posterior constrictions, the middle valley and posterior valley closed on the premolars, protoloph separated from the ectoloph on P2, and buccal and lingual cingula present on premolars, but absent on molars. A phylogenetic analysis reveals that *Tongxinotherium latirhinum* gen. et sp. nov. is more derived than the early elasmotheres, and more primitive than *Iranotherium* and *Ningxiatherium*, bridging a morphological and stratigraphical gap between them. The discovery of new material improves the morphological characteristics of the early elasmotheres' horns and increases the diversity of the middle Miocene elasmotheres.

http://zoobank.org/urn:lsid:zoobank.org:pub:7DF2F57F-38DD-4FBF-B3DF-57AADD510131

Keywords: elasmotheres; middle Miocene; phylogeny; Tongxin; China

Introduction

The elasmotheres, a highly specialized branch of rhinocerotids, were well diversified and widespread in Eurasia and East Africa from the early Miocene to the late Pleistocene (Antoine, 2003; Antoine & Welcomme, 2000; Cerdeño & Nieto, 1995; Deng & Downs, 2002; Geraads et al., 2012, 2016; Handa et al., 2017; Heissig, 1972, 1996, 1999; Schvyreva, 2015; Tong & Moigne, 2000). The earliest elasmothere rhino is *Bugtirhinus praecursor*, which first appeared in South Asia (Pakistan) in the earliest Miocene (Antoine & Welcomme, 2000). In the early Miocene, there were elasmotheres living in Europe and Africa, such as *Hispanotherium* in Western Europe (Antoine et al., 2002; Iñigo & Cerdeño, 1997), *Victoriaceros hooijeri* in Kenya (Geraads et al., 2016) and *Ougandatherium napakense* in Uganda (Guérin & Pickford, 2003). During the middle Miocene, elasmotheres apparently became a more significant component of the large herbivore guild in Western Europe, Asia and Africa, including *Hispanotherium*, *Caementodon*, *Procoelodonta mongoliense* and *Victoriaceros kenyensis* (Antoine, 2003; Antunes, 1979; Antunes & Ginsburg, 1983; Cerdeño, 1992, 1996; Deng, 2003; Deng & Wang, 2004; Ginsburg et al., 1987; Guan, 1988, 1993; Hernández-Pacheco & Crusafont, 1960; Heissig, 1972; Iñigo & Cerdeño, 1997; Yan, 1979; Zhai, 1978). In the late Miocene, elasmotheres diversified and became large terrestrial mammals that inhabited Asia and Africa, especially in China, including *Iranotherium*, *Parelasmotherium*, *Ningxiatherium*, *Sinotherium* and *Elasmotherium* (Chen, 1977; Chow, 1958; Deng, 2001, 2005, 2007; Deng et al., 2013; Killgus, 1923; Mecquenem, 1908; Qiu & Xie, 1998; Ringström, 1923, 1924; Sun et al., 2022), and *Kenyatherium bishopi* and *Samburuceros ishidai* in Kenya (Aguirre & Guerin, 1974; Handa et al., 2017) as well as *Eoazara xerrii* in Morocco (Geraads & Zouhri, 2021). After the late Miocene, elasmotheres became relatively rare. However, elasmotheres appeared in the early Pleistocene in Eurasia, and their existence presumably extended to the late Pleistocene (Kosintsev et al., 2019).

In China, several other elasmotheres from middle Miocene have been described, which are very poorly known, or very incompletely described and illustrated, including *Hispanotherium lintungensis* from Lintong (Zhai,

*Corresponding author. Email: dengtao@ivpp.ac.cn

Published online 18 Aug 2023

1978), *Hispanotherium tungurense* from Inner Mongolia (Cerdeño, 1996), *Tesselodon fangxianensis* from Fangxian (Yan, 1979), *Shennongtherium hyposodontus* from Shennongjia (Huang & Yan, 1983), *Caementodon tongxinensis* from Tongxin (Guan, 1988), *Huaqingtherium qiui* from Tongxin (Guan, 1993), *Procoelodonta mongoliense* from Tongxin (Antoine, 2003), and *Hispanotherium wushanense* from Kangping (Sun et al., 2018). Cerdeño (1996) indicated that *Caementodon tongxinensis* is similar to *Hispanotherium matritense*, which has great intraspecific variation. Deng (2003) demonstrated that *Hispanotherium lintungensis*, *Tesselodon fangxianensis*, *Caementodon tongxinensis* and *Huaqingtherium qiui* are just junior synonyms of *Hispanotherium matritense*, falling well within the variation range of *Hispanotherium matritense*. According to those studies, there were only four representatives of elasmotheres from the middle Miocene in China, including *Hispanotherium matritense*, *Hispanotherium tungurense*, *Hispanotherium wushanense* and *Procoelodonta mongoliense*.

Recently, we discovered an adult elasmothere skull (IVPP V23531) from the middle Miocene of Tongxin, Ningxia. The morphology and geological context of IVPP V23531 impose new constraints upon our understanding of the evolution of early elasmotheres, thereby improving our overall knowledge of the tribe Elasmotheriini. Herein, we describe and compare elasmothere material in detail and discuss its phylogenetic relationships.

Geological background

The Tongxin area is located in the southern part of Wuzhong City, Ningxia Hui Autonomous Region, China. Affected by tectonic activity, there are rich and continuous Cenozoic sediments that have been deposited in the Tongxin area, including the Eocene Sikouzi Formation, the Oligocene Qingshuiying Formation, the lower–middle Miocene Zhang'enbao Formation (previously the Hongliugou Formation), and the upper Miocene Ganhegou Formation.

Zhang'enbao Formation has yielded rich mammal fossils known as the Dingjia'ergou local fauna, dominated by sandstones and siltstones punctuated by mudstones. Heretofore, 14 mammal taxa have been reported, including the lagomorph *Alloptox gobiensis* (Wu et al., 1991), the primate *Pliopithecus zhangxiangi* (Harrison et al., 1991), the carnivore *Tongxinictis primordialis* (Werdelin & Solounias, 1991), *Amphicyon zhanxiangi* (Jiangzuo et al., 2018), *Gobicyon yei* (Jiangzuo et al., 2021), *Oriensmilus liupanensis* (Wang et al., 2020), *Percrocuta xixiaensis* (Xiong, 2022), the proboscidean *Protanancus tobieni* (Wang et al., 2015), *Platybelodon tongxinensis* (Ye & Jia, 1986), *Aphanobelodon zhaoi* (Wang et al., 2017), the suid *Kubanochoerus lantienensis* (Guan & Van der Made, 1993; Qiu et al., 1988), *Bunolistriodon intermedius* (Ye et al., 1992), the crown-antlered deer *Stephanocemas palmatus* (Chen, 1978; Wang et al., 2009), and the elasmothere rhino *Hispanotherium matritense* (Deng, 2003; Guan, 1988, 1993). The fossil sites containing Dingjia'ergou local fauna in the Tongxin area include Yinziling, Gaolingzi, Huangjiashui, Ma'erzuizigou, Baquan, Yuetaizi, Bianqiangou, Gunziling Gou, North Gunziling Gou, South Gunziling Gou, and Yehuquanzi Gou, Miaoerling and Duanbozihang Gou, which are relatively scattered and widely distributed in the fluviolacustrine deposits.

According to Wang et al. (2016), Zhang'enbao Formation is composed of three sections, the lower layers producing more primitive species (i.e. Yinziling sub-fauna), such as *Protanancus tobieni* as well as small and low-crowned *Turcoceros* sp., corresponding to the European Land Mammal Age MN5; the middle layers produced more derived species (i.e. Ma'erzuizigou sub-fauna), such as *Platybelodon tongxinensis* as well as large and high-crowned *Turcoceros* sp., corresponding to the European Land Mammal Age MN6; and the upper layers produced few fossils. Our new elasmothere material reported here was discovered in the middle layers of Zhang'enbao Formation exposed in East Miaoerling in Shishi Township.

Material and methods

This study is based on a skull belonging to an adult individual from Tongxin, Ningxia, housed in the Institute of Vertebrate Paleontology and Paleoanthropology (IVPP), Chinese Academy of Sciences, Beijing, China. Terminology and taxonomy follow Heissig (1972, 1999), Guérin (1980) and Antoine (2002). The specimen was measured according to the procedures described in Guérin (1980).

A phylogenetic analysis was carried out based on morphological characters originally described by Antoine (2002, 2003) with the addition of the new specimen as well as some African elasmotheres (Supplemental material, Files S1, S2) in order to assess the phylogenetic position of the new specimen among elasmotheres. The matrix analysed in the present study contains 282 morphological characters including 52 cranial characters, 120 dental characters and 10 mandibular characters. All multistate characters were treated as additive, except for characters 72, 94, 102, 140 and 187 (non-additive). The phylogenetic analysis was performed via a heuristic search using PAUP4.0a169 (Swofford, 2002), with tree-bisection-reconnection (reconnection limit = 8), 1000 replications with random addition sequence (10 trees held at each step), gaps treated as missing, and no differential weighting or topological constraint a priori. The current matrix consists of 30 taxa coded at the species level with four outgroups (*Tapirus terrestris*, *Ronzotherium filholi*, *Hyrachyus eximius* and *Trigonias osborni*) and 26 in group taxa including 19 elasmotheres (Table 1).

Institutional abbreviations

AMNH, American Museum of Natural History, New York, NY, USA; **HMV**, Hezheng Paleozoological Museum, Gansu, China; **IVPP**, Institute of Vertebrate Paleontology and Paleoanthropology, Chinese Academy of Sciences, Beijing, China; **KNM**, Kenya National Museum, Nairobi, Kenya; **MNCN**, Museo Nacional de Ciencias Naturales, Madrid, Spain; **NHMUK**, Natural History Museum, London, UK.

Systematic palaeontology

Order **Perissodactyla** Owen, 1848
Family **Rhinocerotidae** Owen, 1845
Tribe **Elasmotheriini** Dollo, 1885
Genus ***Tongxinotherium*** gen. nov.

Type and only species. *Tongxinotherium latirhinum* gen. et sp. nov.

Derivation of name. The generic name '*Tongxino*-' from the Tongxin county, where the holotype was discovered; and '*-therium*' from Greek *therion* for wild animal or beast.

Type locality and horizon. As for the type and only species.

Diagnosis. As for the type and only species.

Tongxinotherium latirhinum sp. nov.
(Figs 1–4; Tables 2, 3)

Holotype. IVPP V23531, a slightly dorsoventrally compressed skull with both cheek tooth rows (left and right P2–M3), lacks the occiput (Fig. 1).

Derivation of name. '*Lati*-', from Latin *latus* for broad or wide; '*-rhinum*', from Greek *rhinos* for nose or snout, indicating that this rhino has a very broad nasal bone.

Type locality and horizon. East Miaoerling in Shishi Township, Tongxin County, Wuzhong City, Ningxia Province, China; middle Miocene.

Diagnosis. Relatively large rhinocerotid with wide nasal bone. The dorsal profile of the skull is straight; the rostral end of the nasal bone is very broad, rugose, and thick; the 'U'-shaped nasal notch is located at the level of P3; the anterior margin of the orbit is situated at the level of M2. Teeth are subhypsodont, covered and filled by plentiful cement; enamel foldings are slightly developed; the protocone is expanded, with anterior and posterior constrictions. The protoloph does not join with the ectoloph on P2. On the premolars, the posterior valley is closed; protocone and hypocone are connected leading to the closed middle valley; crochet, crista, and antecrochet are developed. On the molars, the paracone fold is developed; the ectoloph is curved. Buccal and lingual cingula are present on premolars, but absent on molars.

Differential diagnosis. *Tongxinotherium* differs from *Bugtirhinus* in its larger size, with cheek teeth that are covered and filled by plentiful cement while *Bugtirhinus* has relatively rare cement on the cheek teeth. *Tongxinotherium* also differs from *Caementodon* in its larger size; the very broad, rugose and thick rostral end of the nasal bone; and the well-developed crista and lingual cingulum on the premolars. Meanwhile, *Tongxinotherium* is distinguished from *Hispanotherium* in its larger size, even larger than *Hispanotherium tungurense* (the largest species of *Hispanotherium*); the very broad and thick rostral end of the nasal bone; the teeth covered and filled by abundant cement; the curved ectoloph; and the slightly developed enamel foldings. There are apparent differences between *Tongxinotherium* and more advanced elasmotheres including *Iranotherium*, *Parelasmotherium*, *Ningxiatherium*, *Sinotherium* and *Elasmotherium*, such as *Tongxinotherium*'s smaller size, subhypsodont teeth, a shorter skull length, and relatively weak enamel foldings on the cheek teeth. Furthermore, compared with *Ningxiatherium*, *Sinotherium* and *Elasmotherium*, *Tongxinotherium* has an unossified nasal septum, cheek teeth in the posterior part of the skull, and the anterior orbital margin which is at the level of M2. *Tongxinotherium* is distinguished from *Victoriaceros* in the wide nasals, relatively posterior orbital position and a reduced amount of cement on the cheek teeth. *Tongxinotherium* differs from *Kenyatherium* in the well-developed enamel foldings, the expanded protocone with anterior and posterior constrictions, the closed middle and posterior valleys and the developed crochet, crista as well as antecrochet on the premolar, and no lingual cingulum on the molars. *Tongxinotherium* is different from *Samburuceros* in the weak parastyle fold and paracone rib, the closed entrance of the medial valley on M1, and well-developed and stronger crochet. *Tongxinotherium* is distinguished from *Eoazara* in having a very broad, rugose, and thick rostral end of the nasal bone, and the relatively weaker anterior and posterior constrictions of protocone.

Table 1. Taxa used in the phylogenetic analyses.

Taxon	Temporal distribution	Geographical distribution	Source of character scores
Brachypotherium brachypus (Lartet, 1837)	middle Miocene	Eurasia	Original scoring of Antoine (2003)
Bugtirhinus praecursor Antoine and Welcomme, 2000	early Miocene	Pakistan	Original scoring of Antoine (2003)
Diceratherium armatum Marsh, 1875	late Oligocene to early Miocene	North America	Original scoring of Antoine (2003)
Caementodon caucasicum (Borissiak, 1935)	middle Miocene	Caucasus	Original scoring of Antoine (2003)
Eoazara xerrii Geraads and Zouhri, 2021	late Miocene	North Africa	Geraads and Zouhri, 2021
Elasmotherium caucasicum Borissiak, 1914	Pleistocene	North and Central Asia	Original scoring of Antoine (2003)
Elasmotherium primigenius Sun et al., 2021	late Miocene	China	Original scoring of Sun et al. (2021)
Elasmotherium sibiricum Fischer, 1808	Pleistocene	Siberia	Original scoring of Antoine (2003)
Hispanotherium matritense (Prado, 1864)	middle Miocene	Eurasia	Original scoring of Antoine (2003)
Hispanotherium tungurense Cerdeño (1996)	middle Miocene	China	Original scoring of Antoine (2003)
Hyrachyus eximius Leidy, 1871	Eocene	North America	Original scoring of Antoine (2003)
Kenyatherium bishopi Aguirre and Guérin, 1974	early Miocene	Kenya	Original scoring of Antoine (2003)
Iranotherium morgani (Mecquenem, 1908)	late Miocene	China	Original scoring of Deng (2008)
Menoceras arikarense (Barbour, 1906)	early Miocene	North America	Original scoring of Antoine (2003)
Ningxiatherium longirhinus Chen, 1977	late Miocene	China	Original scoring of Deng (2008)
Ougandatherium napakense Guérin and Pickford 2003	early Miocene	Napak	Guérin and Pickford, 2003
Parelasmotherium schansiense Killgus, 1923	late Miocene	China	Original scoring of Antoine (2003)
Parelasmotherium linxiaense Deng, 2001	late Miocene	China	Original scoring of Deng (2008)
Plesiaceratherium mirallesi (Crusafont, Villalta and Truyols, 1955)	early Miocene	Spain, France	Original scoring of Deng (2008)
Prosantorhinus douvillei (Osborn, 1900)	early Miocene to middle Miocene	Europe	Original scoring of Antoine (2003)
Procoelodonta mongoliense (Osborn, 1924)	middle Miocene	China, Mongolia	Original scoring of Antoine (2003)
Protaceratherium minutum (Cuvier, 1822)	late Oligocene to early Miocene	Europe	Original scoring of Deng (2008)
Ronzotherium filholi (Osborn, 1900)	Oligocene	Europe	Original scoring of Antoine (2003)
Samburuceros ishidai Handa et al., 2017	early late Miocene	Kenya	Handa *et al.* 2017
Sinotherium lagrelii Ringström, 1922	late Miocene	China	Original scoring of Deng (2008)
Tapirus terrestris (von Linnaeus, 1758)	late Pleistocene to present	North America	Original scoring of Antoine (2003)
Teleoceras fossiger (Cope, 1878)	early Miocene	North America	Original scoring of Antoine (2003)
Tongxinotherium latirhinum gen. et sp. nov.	middle Miocene	China	Direct observation
Trigonias osborni Lucas, 1900	late Eocene to early Oligocene	North America	Original scoring of Antoine (2003)
Victoriaceros kenyensis Geraads et al., 2012	middle Miocene	Kenya	Geraads *et al.* 2012, 2016

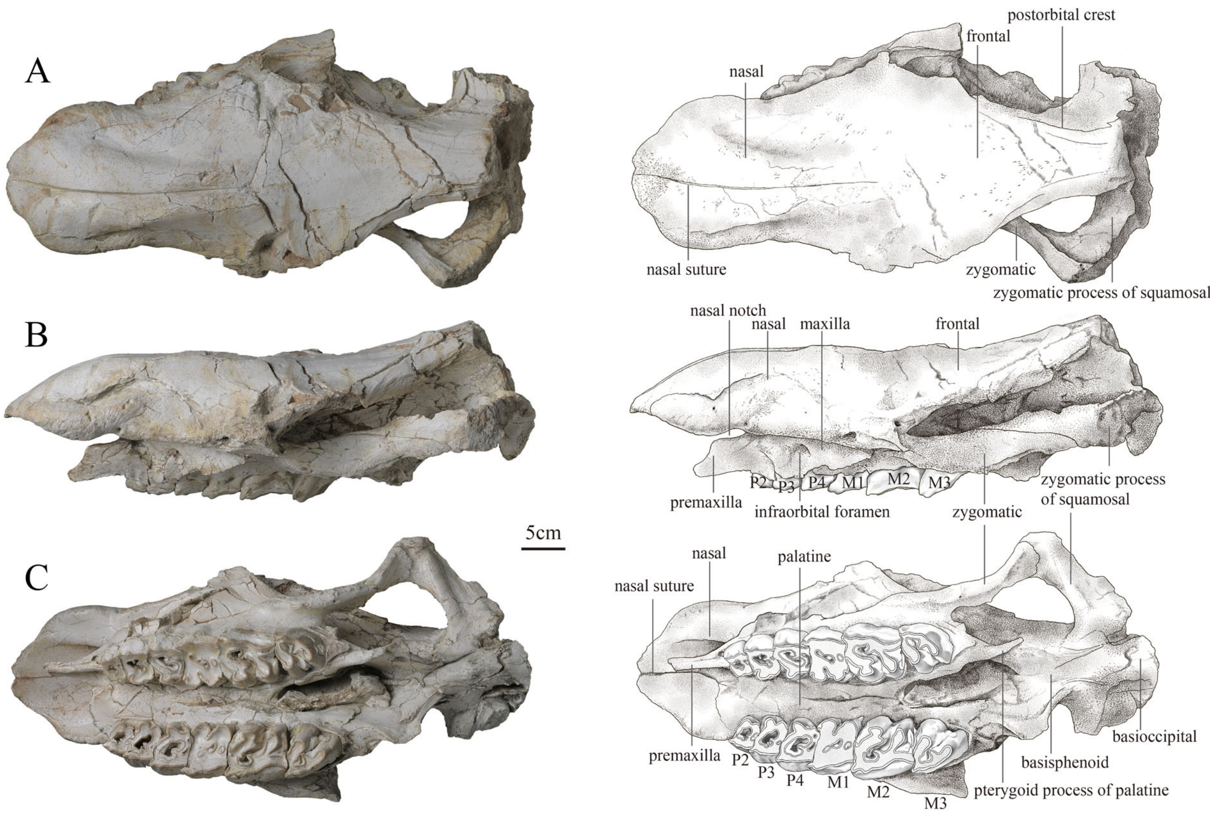

Figure 1. Photographs and sketches of the skull of *Tongxinotherium latirhinum* gen. et sp. nov., holotype (IVPP V23531): **A,** dorsal view; **B,** lateral view; **C,** ventral view.

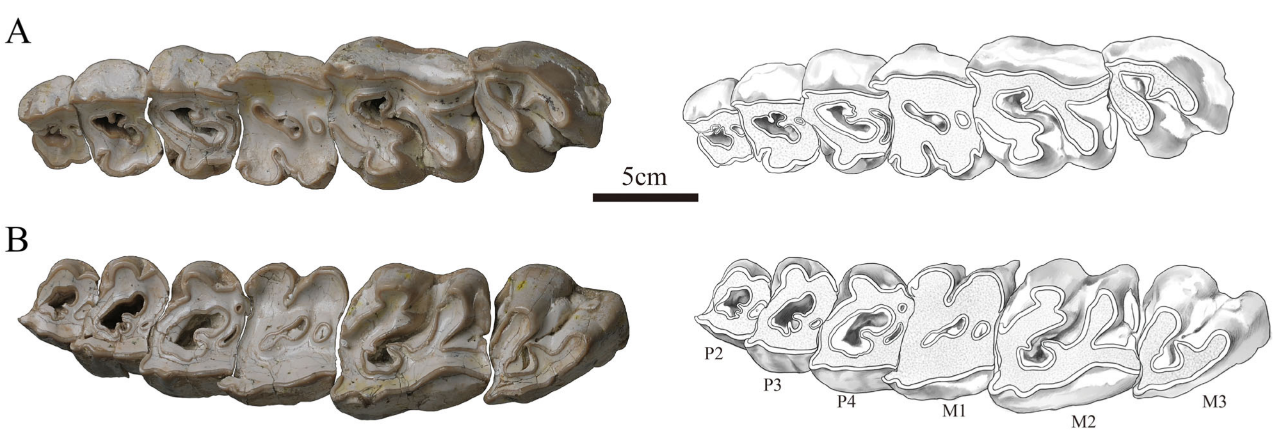

Figure 2. Photographs and sketches of the teeth of *Tongxinotherium latirhinum* gen. et sp. nov. in occlusal view, holotype (IVPP V23531): **A,** left view; **B,** right view.

Description

IVPP V23531 is a full adult skull with moderately worn cheek teeth, lacking part of the premaxilla, the occiput as well as part of the zygomatic bone. The material is only slightly dorsoventrally compressed, so the morphologies of the dorsal profile of the skull, the nasal bone width, and the nasal notch position have been very

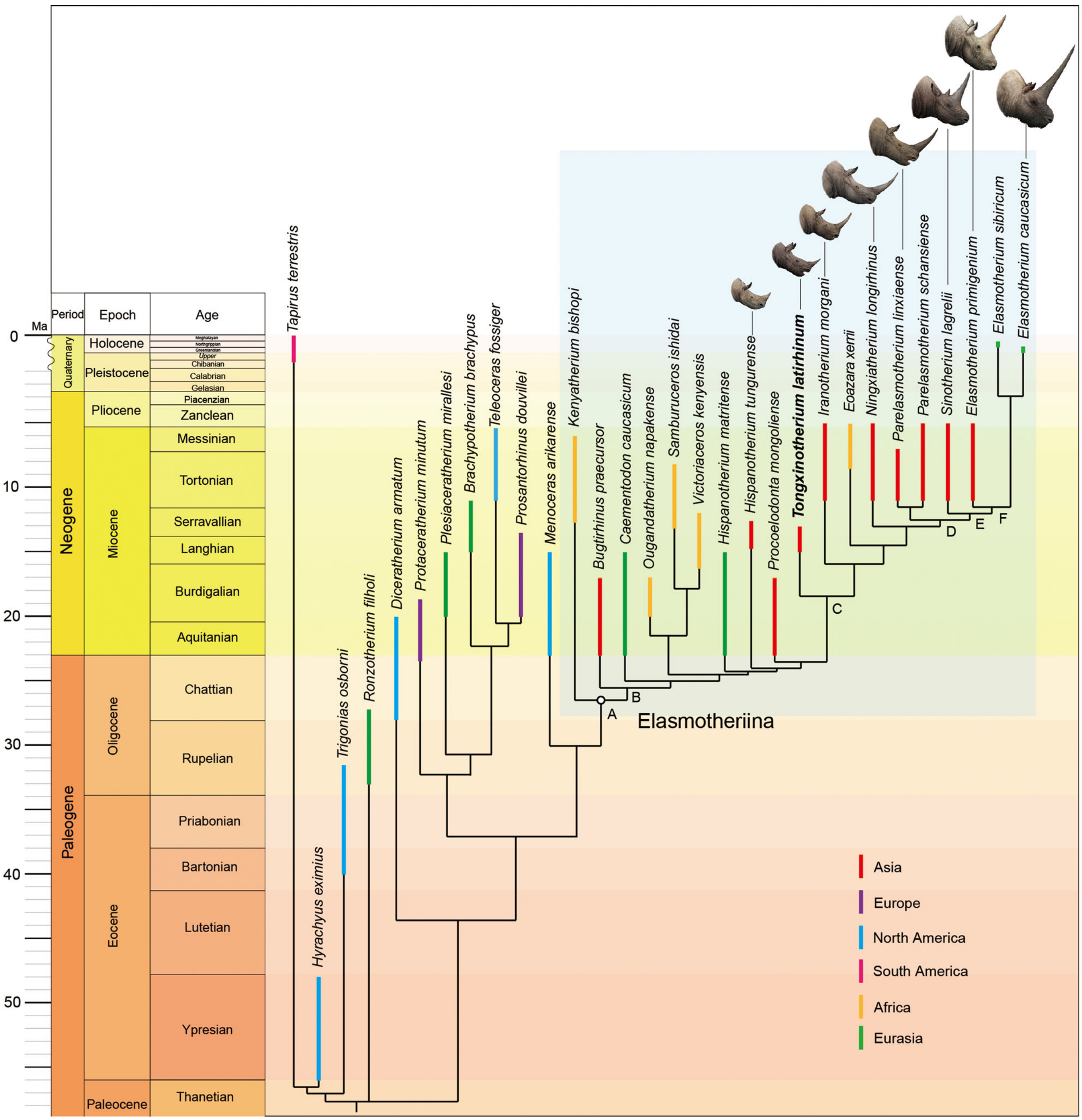

Figure 3. Most parsimonious tree showing phylogenetic positions of *Tongxinotherium latirhinum* gen. et sp. nov. within elasmotheres. For convenience, capital letters (A–F) below the branches are used to denote monophyletic groups discussed in the text. The skulls are reconstructed based on AMNH 26531 (Tunggur in Inner Mongolia, middle Miocene) for *Hispanotherium tungurense*, IVPP V23531 (East Miaoerling in Tongxin, Ningxia, middle Miocene) for *Tongxinotherium latirhinum* sp. nov., HMV 0979 (Houshan in Guanghe, Gansu, late Miocene) for *Iranotherium morgani*, HMV 1411 (Guonigou in Dongxiang, Gansu, late Miocene) for *Parelasmotherium linxiaense*, HMV 1449 (Guonigou in Dongxiang, Gansu, late Miocene) for *Ningxiatherium euryrhinus*, IVPP V18539 (Huaigou in Guanghe, Gansu, late Miocene) for *Sinotherium lagrelii*, IVPP V24051 (Yangjing in Dingbian, Shaanxi, late Miocene) for *Elasmotherium primigenium*, and NHMUK PV M12429 (Sarepta in Russia, late Pleistocene) for *Elasmotherium sibiricum.*

subtly affected by this deformation. The skull is dolichocephalic. The dorsal profile of the skull is nearly straight. The skull roof is the widest at the level of the lacrimal tubercle, being 260.02 mm. The nasal bone narrows gradually before the orbits, i.e. the nasal base does not have a constriction. The nasal bone is fused, and the rostral end of the nasal bone is very broad, rugose, and thick, which indicates there is a medial

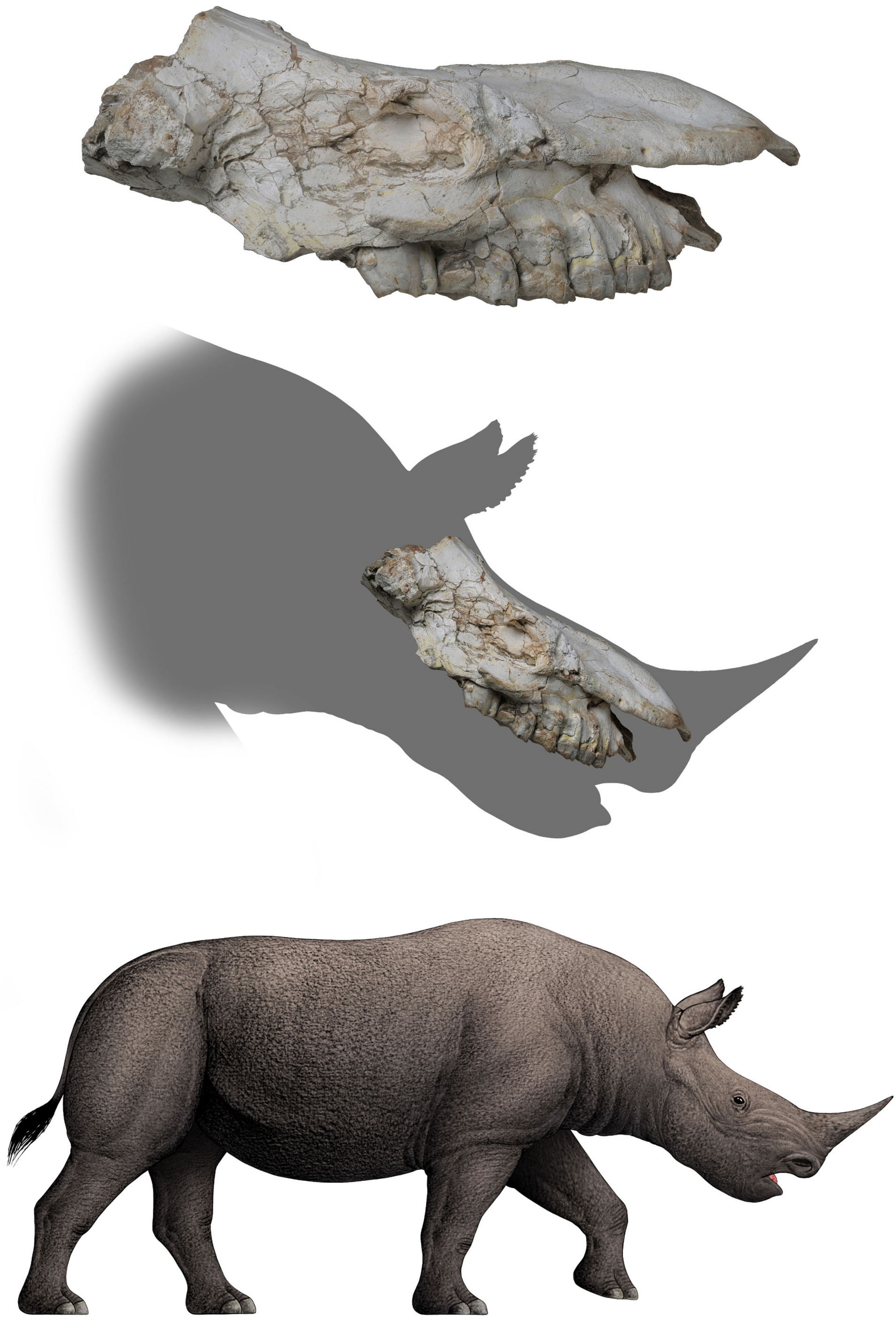

nasal horn here. The nasal notch outline is ‘U’-shaped and its posterior edge is located at the level of P3. The distance between the posterior edge of the nasal notch and the orbit is 165.72 mm. The infraorbital foramen is located dorsal to the level of P4 and behind the nasal notch. The position of the dorsal margin of the orbit is high, and the anterior margin of the orbit is located anteroposteriorly, near the middle of M2. The zygomatic arch is fairly thin (particularly the posterior part), the anterior end of which is located at the level of M2 with the dorsal margin curved. The postorbital processes on the frontal and zygomatic bones are comparatively weak. The palatal surface is smooth and widely arched. The lacrimal tubercle is developed. The foramen sphenorbitale and foramen rotundum are fused. The anterior rim of the choanae is ‘U’-shaped; the ventral ridge of the vomer is acute; the posterior edge of the pterygoid is nearly vertical. The articular tubercle of the squamosal is smooth, and the transverse profile is straight; the cross-section of postglenoid processes is prismatic. The basilar tubercles are well developed. The basicranium part is poorly preserved. The postglenoid process is broken, only the base is preserved. The temporal condyle is flat and straight. The glenoid cavity is deep. The occipital crest is broken.

Upper cheek teeth

Only a portion of the premaxilla was preserved, so we cannot directly observe whether there is a slot retained for I1. The dental formula is ?0·4·3. The premolars and molars are moderately worn (Fig. 2). The upper cheek tooth row is almost oriented in a straight line located in the posterior portion of the cranium relative to the orbit. The ratio of the length of upper premolars (P3–4) to the molars (M1–3) is low, 47%. On the upper cheek teeth, the cement on the buccal surface is fairly well developed; the buccal wall is curved; the lingual cusps are expanded; the protocone is anteroposteriorly constricted; the enamel foldings are weak; the branch of the crochet is occasionally present. On the premolars, the medial valley is closed; the protocone is constricted, and its lingual margin is curved. On the molars, the antecrochet is developed and the antecrochet fold spreads to the entrance of the median valley; the crochet and crista are developed; the buccal and lingual cingula are absent; the protocone is strongly constricted, and its lingual margin is straight.

DP1 is not preserved. From the size of the opening for the tooth root, the DP1 is fairly small. The outline of P2 is nearly quadrangular in occlusal view with a parastyle and comparatively weak parastyle fold. The protocone and hypocone connect with each other by a lingual wall without constriction. The hypocone is larger than the protocone. The hypocone is oriented posteriorly, as is the metacone. The protoloph is as buccally narrow as the metaloph and does not join with the ectoloph. The crochet and crista are well developed. Both the medial valley and the posterior valley are closed. The lingual cingulum is weak, forming a ‘V’-shaped incision around the entrance of the median valley. The buccal cingulum is absent. The cement on the buccal surface is abundant.

P3 has a slightly projecting parastyle, with a marked parastyle fold and paracone rib. As a result, the buccal wall is curved. The protocone is expanded, with anterior and posterior constrictions, while the hypocone only has a slight anterior constriction. The protocone and hypocone connect with each other by a lingual wall. The protocone is larger than the hypocone. The crochet and crista are well developed. The medial and posterior valleys are closed. The lingual margin of the protocone is curved. The lingual cingulum is weak, and forms a ‘V’-shaped incision around the entrance of the median valley. The buccal cingulum is absent. P4 is similar to P3, but much larger. The hypocone is not expanded, having a slight anterior constriction. The protocone is slightly larger than the hypocone. The lingual margin of the protocone is curved.

M1 is deeply worn. It has a projecting parastyle, with a marked parastyle fold and paracone rib, so the buccal wall is curved. The strongly constricted protocone has a flat lingual margin, and the hypocone only has a slight anterior constriction. The medial valley leans posteriorly, which is narrow and closed. The posterior valley is round in shape and closed. The lingual and buccal cingula are absent.

M2 has a narrow and long parastyle and a developed parastyle fold and paracone rib. It has slightly developed anterior and posterior cingula but no lingual cingulum. The protocone is expanded, with anterior and posterior constrictions. The hypocone only has a slight anterior constriction. The crochet and crista are well developed. The antecrochet is strongly developed, and the sharp end extends to the entrance of the medial valley. The antecrochet and hypocone are separated. It has an open medial valley, a ‘V’-shaped posterior valley, a relatively narrow and long metastyle, and a deep depression on the buccal wall of the metacone.

M3 is triangular in occlusal view because the ectoloph and metaloph are fused. It has a short and sharp parastyle, a wide protoloph, and an ectometaloph. The

Figure 4. Reconstruction of *Tongxinotherium latirhinum* gen. et sp. nov.

Table 2. Measurements of the skull of *Tongxinotherium latirhinum* gen. et sp. nov. compared with other elasmotheres (mm). The numbers in front of the features measured correspond to those of Guérin (1980, p. 47, table 1).

	Features measured	*T. latirhinum* IVPP V23531	*H. matritense* MNCN05/101/2/7000	*I. morgani* HMV0979,1098	*P. linxiaense* HMV 1411	*N. euryrhinus* HMV 1449	*N. longirhinus* IVPP V 5163
1	Distance between occipital condyle and premaxilla	556.32	—	712–775	925	875	864
2	Distance between occipital condyle and nasal tip	612.12	—	700–745	1015	985	904
3	Distance between nasal tip and occipital crest	—	—	710–750	973	1010	935
4	Distance between nasal tip and bottom of nasal notch	155.87	—	145–176	369	318	267.7
5	Minimal width of braincase	115.5	105	123–140	166	190	146
6	Distance between occipital crest and postorbital process	—	—	310–348	365	390	349.5
7	Distance between occipital crest and supraorbital process	—	—	355–380	420	425	381
8	Distance between occipital crest and lacrimal tubercle	—	—	390–453	~450	475	456
9	Distance between nasal notch and orbit	165.72	113	216–204.5	217	268	259.4
13	Distance between occipital condyle and M3	237.59	—	330–395	438	450	445
14	Distance between nasal tip and orbit	316.41	—	350–375	565	570	521
15	Width of occipital crest	—	—	190–212.4	183	224	205
16	Width of paramastoid process	—	190	251–309	306	379	268
17	Minimal width between parietal crests	83.29	11	80–91	113.6	121	108.4
18	Width between postorbital processes	193.21	151	211–244	228	270	222
19	Width between supraorbital processes	209.36	—	253–260	231.5	282	~248
20	Width between lacrimal tubercles	260.02	165	282–295	~207	400	~284
21	Maximal width between zygomatic arches	287.06	284	340–420	—	460	360
22	Width of nasal base	160.52	65	117–140	158.4	235	134.5
23	Height of occipital surface	—	—	137–138	193.5	154.5	212
25	Cranial height in front of P2	160.65	150	173–193	232.7	137	281
26	Cranial height in front of M1	167.18	189	180–251	237.3	154	279
27	Cranial height in front of M3	156.55	—	196–259	240	144	260
28	Width of palate in front of P2	48.44	—	67–68	96.8	139	49.6
29	Width of palate in front of M1	54.46	—	68–93	104	140	79
30	Width of palate in front of M3	62.89	—	77–131	125	160	90
31	Width of foramen magnum	—	40	44–57	88	71	71.7
32	Width between exterior edges of occipital condyle	—	118	133–183	186	215	181.4

Table 3. Measurements of the upper teeth of *Tongxinotherium latirhinum* gen. et sp. nov. compared with other elasmotheres (mm).

Teeth		*T. latirhinum* IVPP V23531	*C. oettingenae* (Heissig, 1972)	*C. tongxinensis* (Guan, 1988, 1993)	*H. lintungensis* (Zhai, 1978)	*H. matritense* (Deng, 2003)	*H. tungurense* (Cerdeño, 1996)	*T. fangxianensis* (Deng, 2003)
P2	L	28.51	23	–	25.1	–	26.2	17
	W	33.59	27–28	–	33.2	–	30.5	16
	H	25.11		–	–	–	–	21
P3	L	32.57	26	–	25.5	30	34.2	29
	W	44.82	33–35	–	41.5	41	41.8	32.7
	H	26.28		–	–	38	–	30.5
P4	L	38.64		29.6	26	33.5	36.1–39.4	30
	W	48.33		39	44.7	45.5	47.2–57.9	37
	H	28.42		36.3	–	44.5	–	49
M1	L	49.61	34	38.9	33.3	44	42.5–48.9	–
	W	58.94	41–42	46.2	50.5	52.5	59.2–64.4	–
	H	24.32		33.8	–	44	–	–
M2	L	66.67	43	45.7	49	49/56/54. 5	60.9–64.6	–
	W	50.69	42–45	45.7	59.6	57/55/56. 5	63.5–73.1	50.3
	H	35.32		–	–	44/58.5/63.6	–	56
M3	L	49.78	44	45.7	45.7	49.5/47/48	46.4–60	–
	W	40.75	30	47.1	53.3	50/49.5/50.5	56.6–67.5	–
	H	39.22		60	–	30/50/70	–	–

protoloph is transverse on the anterolingual side. The crochet is well developed but does not form a medifossette. The protocone has anterior and posterior constrictions. The anterior cingulum is well developed.

Comparisons

The specimen (IVPP V23531) from Tongxin, Ningxia shares the following synapomorphies of the Tribe Elasmotheriini (Antoine, 2002; Heissig, 1972): the cheek teeth are covered and filled by plentiful cement; enamel foldings are slightly developed; the protocone has anterior and posterior constrictions; on the premolars, a lingual wall is developed, the middle and posterior valleys are closed, and the crochet, crista, as well as antecrochet are well developed.

As mentioned above, there are few previous studies on rhinoceros fossils from the middle Miocene in the Tongxin area. Guan's (1988, 1993) reports on elasmothere rhinos were previously revised by Cerdeño (1996) and Deng (2003). In addition, Antoine (2003) mentioned that *Procoelodonta mongoliense* was also discovered from the early middle Miocene of Tongxin, China. Therefore, only two representatives (i.e. *Hispanotherium matritense*, *Procoelodonta mongoliense*) of rhinoceroses from the middle Miocene are recognized in Tongxin, Ningxia.

Hispanotherium matritense is a small-sized elasmothere, possessing subhypsodont cheek teeth with a very thick cement cover, upper premolars with a closed median valley, and well-developed secondary folds of the enamel (Cerdeño, 1992; Iñigo & Cerdeño, 1997; Sanisidro et al., 2012). The Tongxin specimen is distinguished from *H. matritense* in its larger size. The nasal bones of the Tongxin specimen are very broad and thick, whereas those of *H. matritense* are narrow and thin. The nasal notch of the Tongxin specimen is located at the level of P3 while the notch of *H. matritense* reaches the level of P4. The anterior margin of the orbit of the Tongxin specimen is situated at the level of M2, whereas that of *H. matritense* is situated at the level of M3. The enamel foldings of the Tongxin specimen are slightly developed, while those of *H. matritense* are well developed. Therefore, the Tongxin specimen differs from *H. matritense* in several morphological features.

Compared with *P. mongoliense* (Antoine, 2003), the two species have significant differences as follows. The nasal bones of *P. mongoliense* are narrow and strongly curved in anterior view, forming a high axial vertical ridge, whereas those of the Tongxin specimen are very broad and slightly curved in anterior view. The anterior margin of the orbit of the Tongxin specimen is situated at the level of M2, whereas that of *P. mongoliense* is situated at the level of M1. The enamel foldings of the Tongxin specimen are slightly developed but there are no secondary folds developed on teeth of *P. mongoliense.* In addition, the lingual cingulum of the Tongxin specimen is weak, forming a 'V'-shaped incision around the entrance of the median valley, whereas that of *P. mongoliense* is absent.

In addition, *Hispanotherium tungurense* from the middle Miocene of Tung Gur in Inner Mongolia, described based on both cranial and postcranial remains (Cerdeño, 1996), is geographically quite close to the Tongxin specimen. *Hispanotherium tungurense* with a developed nasal horn boss is larger than other species previously assigned to *Hispanotherium*. Comparing the Tongxin specimen and *H. tungurense*, there are some similarities between the two species. The infraorbital foramen of both species is located dorsal to the level of P4 and the anterior margin of the orbit of both species is situated at the level of M2. However, there are also distinct differences between the two species. The nasal bones of *H. tungurense* are comparatively narrow and thin, whereas those of the Tongxin specimen are very broad and thick. The enamel foldings of *H. tungurense* are well developed compared to those of the Tongxin specimen, which are slightly developed. The constrictions of the protocone on M3 of *H. tungurense* are more strongly developed than those of the Tongxin specimen. The ectoloph on upper teeth of *H. tungurense* is more undulated than that of the Tongxin specimen. Moreover, Sun et al. (2018) described a new species of *Hispanotherium*, *H. wushanense*, based on a left maxillary fragment with M2 and M3. Due to the scarcity of the material, further study is needed to determine the validity of *H. wushanense*. Therefore, no comparison is made here.

In addition, numerous Eurasian sites have also yielded abundant materials of Elasmotheriini. Antoine and Welcomme (2000) established a new genus and species, *Bugtirhinus praecursor* from the early Miocene of Pakistan, based on several teeth and postcranial bones. Localities with *B. praecursor* correspond to the lower part of the MN 3 and *B. praecursor* is the earliest representative of the elasmotheres. It is very small in size, being even smaller than *Caementodon oettingenae*, and it exhibits great differences from the Tongxin specimen. For the Tongxin specimen, the cheek teeth are covered and filled by plentiful cement, while *B. praecursor* has relatively rare cement on the cheek teeth; the metaloph on M1 and M2 is longer than that of *B. praecursor*; and the parastyle fold and paracone rib are a little weaker than those of *B. praecursor*, as is the mesostyle.

Caementodon was established by Heissig (1972) based on teeth and postcranial materials in the Chinji layer of Sivalik. The type species, *Caementodon oettingenae*, is a small primitive elasmothere with abundant cement on the cheek teeth. The Tongxin specimen is larger than *C. oettingenae*. The outer walls of the upper cheek teeth of the Tongxin specimen are relatively wavy while those of *C. oettingenae* are straight. The skulls of *Bugtirhinus* and *Caementodon* are unknown, so we can only compare the differences in teeth. In general, the Tongxin specimen is bigger than the early elasmotheres, such as *Bugtirhinus*, *Caementodon* and *Hispanotherium*, having no lingual cingulum on the upper molars, weaker parastyle fold and paracone rib, and plentiful cement cover and filling.

In the late Miocene of Eurasia, elasmotheres diversified and became large terrestrial mammals. Ringström (1924) referred *Rhinoceros morgani* from the late Miocene of Maragheh in Iran as a new genus, *Iranotherium*. Deng (2005) reported the same species from the late Miocene of the Linxia Basin, China. *Iranotherium morgani* is a large rhinocerotid with a big nasal horn and hypsodont teeth, while the Tongxin specimen is smaller than *I. morgani*, and has a relatively smaller nasal horn and subhypsodont teeth. The enamel foldings of *I. morgani* are well developed while those of the Tongxin specimen are slightly developed. The constrictions of protocone on M3 of *I. morgani* are more developed than those of the Tongxin specimen. *Iranotherium morgani* has a shallow nasal notch located at the level of P2/P3 boundary and the anterior margin of orbit situated at the level of M3, whereas the 'U'-shaped nasal notch of the Tongxin specimen is located at the level of P3 and the anterior margin of the orbit is situated at the level of M2.

Killgus (1923) described *Parelasmotherium schansiense* based on several upper cheek teeth from the late Miocene of Shanxi. Qiu and Xie (1998) referred *Sinotherium simplum* to *Parelasmotherium simplum* (Chow, 1958). Deng (2001) erected a new species *Parelasmotherium linxiaense* from the late Miocene of the Linxia Basin based on upper molars. Later, Deng (2007) described skull material from the Linxia Basin as *P. linxiaense*. So far, the *Parelasmotherium* is only found in China. The Tongxin specimen differs from *Parelasmotherium* in its smaller size. *Parelasmotherium linxiaense* has a rough and large nasal horn boss without a frontal horn, while the Tongxin specimen has a relatively smaller nasal horn boss. The nasal notch of *P. linxiaense* is deep above M1, whereas that of the Tongxin specimen is shallow. *Parelasmotherium linxiaense* has hypsodont cheek teeth, wrinkled enamel, well-developed crista and expanded hypocone, however the Tongxin specimen has relatively weak enamel foldings on the cheek teeth. Hence, *Parelasmotherium* is more derived than the Tongxin specimen.

Chen (1977) established the genus *Ningxiatherium* based on a complete skull with upper cheek tooth rows from P4 to M3 from an old individual from the late Miocene of Zhongning, Ningxia in China. Ringström (1923) established the genus *Sinotherium* from the Baodean of China. This is a highly specialized taxon with a huge nasofrontal horn, short and deep face, large and hypsodont cheek teeth, and wrinkled enamel (Deng et al., 2013; Ringström, 1924). The genus *Elasmotherium* was named by Fischer (1808) based on materials discovered in Siberia, hence the type species *E. sibiricum*. Compared with *Ningxiatherium*, *Sinotherium* and *Elasmotherium*, *Tongxinotherium* is more primitive than the relatively large elasmotheres in its smaller size with a shorter length of the skull, unossified nasal septum, cheek teeth which are in the posterior part of the skull, and the anterior orbital margin which is at the level of M2.

Except for Eurasia, there are many species of Elasmotheriini that have been discovered from Africa. Geraads et al. (2012) established the genus *Victoriaceros* based on an almost completely preserved skull found from Maboko in Kenya, with the type species being *V. kenyensis*. Geraads et al. (2016) tentatively assigned a skull from Karungu in Kenya to another species of *Victoriaceros*, *V. hooijeri*, and they regarded the genus *Victoriaceros* as close to the Elasmotheriinae, if not a member of this subfamily. The Tongxin specimen obviously differs from the crania of both species in their narrow nasals, relatively anterior orbital position, probable presence of upper incisors, and plentiful cement on the cheek teeth.

Aguirre and Guerin (1974) described two upper teeth (P4 and M1) from the late Miocene of Kenya as a new Elasmotheriini species, *Kenyatherium bishopi*. Nakaya et al. (1987) and Handa (2016) identified some isolated upper molars as *K. bishopi*. The Tongxin specimen differs from *K. bishopi* in the following: the enamel foldings are more slightly developed than those of *K. bishopi*; the protocone is expanded, with anterior and posterior constrictions, while that of *K. bishopi* shows the normal state, being unexpanded, only with constrictions; on the premolars, the middle and posterior valleys are closed, and the crochet, crista as well as antecrochet are developed, however, the posterior valley of *K. bishopi* is open, and the crochet is weaker; the protocone and hypocone are more strongly constricted than those of *K. bishopi*; there is no lingual cingulum on the molars, whereas *K. bishopi* has a reduced lingual cingulum.

Handa et al. (2017) described a few upper molars, a maxillary fragment, and two mandibular fragments from early late Miocene of Nakali, Kenya, and erected a new genus *Samburuceros* whose type species is *S. ishidai*. As part of the differences between the two species, the parastyle fold and paracone rib of the Tongxin specimen are not as strong as those of *S. ishidai*. The entrance of the medial valley on M1 of the Tongxin specimen is closed by the connection of the protocone and hypocone while that of *S. ishidai* is open. The protocone and hypocone of *S. ishidai* are more strongly constricted than those of the Tongxin specimen. Unlike *S. ishidai*, the crochet of the Tongxin specimen is well developed and stronger.

Geraads & Zouhri (2021) established a new genus and new species, *Eoazara xerrii* from the late Miocene of Skoura in North Africa, based on a virtually complete skull with articulated mandible and a few fragmentary postcranial remains. *Eoazara xerrii* is characterized by long nasal bones with a strong horn base, long and edentulous premaxillae, and prominent orbital rim. *Eoazara xerrii* has stronger anterior and posterior constrictions of the protocone than that of the Tongxin specimen. Moreover, the latter has a very broad, rugose, and thick rostral end of the nasal bone.

Phylogenetic analysis

In order to further discuss the diagnostic characters of the new genus and species from Tongxin, *Tongxinotherium latirhinum*, we conducted a phylogenetic analysis using PAUP4.0a169 (Swofford, 2002), resulting in a most parsimonious tree (Fig. 3). The tree length is 1020 steps, with a consistency index of 0.3627 and a retention index of 0.5715. *Brachypotherium brachypus*, *Prosantorhinus douvillei* and *Teleoceras fossiger*, members of Teleoceratini, are part of a stable clade. *Menoceras arikarense* is the sister-group of Elasmotheriina (i.e. Elasmotheriines *sensu stricto*) which is consistent with the results of Antoine's (2003) phylogenetic analysis. However, the position of *Diceratherium* is tentative and needs further study. The clade containing all groups of Elasmotheriina (Node A) is supported by 32 equivocal synapomorphies: the processus postorbitalis on squamosal (ch. 13^{0-1}), posterior margin of pterygoid nearly horizontal (ch. 22^{1-0}), median nasal horn present (ch. 27^{0-1}), vomer acute (ch. 38^{1-0}), processus postglenoidalis of squamosal flat (ch. 42^{1-0}), the radio of compared length of the premolars/-molars rows between 42% to 50% (ch. 63^{0-1}), cheek teeth crown high (ch. 68^{0-1}), postfossette of P2–4 narrow (ch. 89^{0-1}), protocone and hypocone of P2 with a lingual wall (ch. 94^{1-3}), hypocone of P2 posterior to metacone (ch. 95^{0-1}), medifossette of P3–4 always absent (ch. 100^{1-0}), protocone and hypocone of P3–4 separated (ch. 102^{2-3}), separate crista of P3 always absent (ch. 105^{1-0}), constriction of the protocone of M1–2 strong (ch. 116^{0-1}), constriction of the protocone of M3 always present (ch. 135^{0-2}), lingual cingulum of lower premolars usually absent (ch. 147^{0-2}), labial cingulum of the lower premolars absent (ch. 149^{0-1}), lingual cingulum of the lower molars usually present (ch. 157^{0-1}), di2 absent (ch. 171^{0-1}), ectolophid fold of d2–3 absent (ch. 177^{0-1}), anterior groove on the ectolophid of d2 present (ch. 178^{0-1}), greater trochanter of humerus low (ch. 192^{0-1}), fossa olecrani of the humerus low (ch. 193^{0-1}), anterior border of the proximal articulation of the radius 'M'-shaped (ch. 197^{0-1}), insertion of the m. biceps brachii of the radius shallow (ch. 200^{0-1}), angle between the diaphysis and olecranon of the ulna open (ch. 205^{0-1}), distal facet for the semilunate of the pyramidal symmetric (ch. 214^{1-0}), proximal border of the trapezoid asymmetric in anterior view (ch. 216^{0-1}), the fovea capitis of the femur high and narrow (ch. 238^{1-0}), anterodistal groove of the tibia absent (ch. 242^{0-1}), tibia-fibula in contact or fused (ch. 245^{0-1}), laterodistal gutter of the fibula deep (ch. 250^{0-1}), posteroproximal tuberosity of the MtIV pad-shaped and continuous (ch. 277^{0-1}). Node B is supported by five equivocal synapomorphies: the labial cingulum of upper premolars is usually absent (ch. 83^{3-2}), the crochet of P2–4 is always simple (ch. 85^{2-0}), the lingual cingulum of P2–4 is always absent (ch. 87^{0-3}), the protocone of P2 is less strong than the hypocone (ch. 101^{3-1}), the lingual cingulum of upper molars is usually absent (ch. 114^{0-1}).

Since the fossil materials of *Procoelodonta* are scarce, it is unknown whether *Procoelodonta* played a key role in the evolution of elasmotheres, and its taxonomy needs to be further studied. The new genus *Tongxinotherium* established here forms a branch (Node C) with other advanced elasmotheres, and its taxonomic position is consistent with the analysis of specific characteristics. Node C is supported by eight equivocal synapomorphies: processus postorbitalis of zygomatic arch present (ch. 12^{0-1}), enamel folding of cheek teeth weak (ch. 64^{0-1}), labial cingulum of upper molars always absent (ch. 109^{2-3}), metacone fold of M1–2 absent (ch. 119^{0-1}), cristella of M1–2 present (ch. 123^{0-1}), antecrochet-hypocone of M1 joined (ch. 126^{2-1}), mesostyle of M2 absent (ch. 130^{1-0}), protocone of M3 indented (ch. 136^{0-1}). *Tongxinotherium latirhinum* is large, with a broad and thick nasal bone, supported by 12 equivocal synapomorphies: zygomatic arch low (ch. 11^{1-0}), dorsal profile of the skull flat (ch. 15^{1-0}), the posterior margin of the pterygoid nearly vertical (ch. 22^{0-1}), enamel of cheek teeth wrinkled (ch. 67^{2-0}), lingual cingulum of P2–4 always present (ch. 87^{3-0}), lingual cingulum of P2–4 continuous (ch. 89^{1-0}), protoloph of P2 not connected to the ectoloph (ch. 99^{0-1}), lingual cingulum of upper molars usually absent (ch. 114^{3-2}), metaloph of M1–2 long (ch. 121^{1-0}), metaloph of M1 continuous ch. (125^{1-0}), metaloph of M2 continuous (ch. 129^{1-0}), posterior groove on the ectometaloph of M3 absent (ch. 138^{0-1}). *Parelasmotherium* and *Sinotherium*-*Elasmotherium* form sister taxa, and their nearest common ancestor is at Node D which is supported by 13 equivocal synapomorphies: zygomatic arch low (ch. 11^{1-0}), area between temporal and nuchal crests flattened (ch. 17^{1-0}), occipital face vertical (ch. 19^{2-1}), occipital crest straight (ch. 36^{0-1}), anterior base of the zygomatic arch strong (ch. 37^{0-1}), the radio of compared length of the premolars/molars rows is less than 42% (ch. 63^{2-1}), crown of cheek teeth shows subhypsodonty (ch. 69^{1-2}), the crochet of P2–4 present (ch. 84^{2-1}), the crochet of upper molars usually absent (ch. 111^{2-1}), crista of upper molars present (ch. 112^{2-3}), paracone fold of M1–2 present (ch. 117^{1-0}), antecrochet and hypocone of M1 separated (ch. 126^{1-0}), antecrochet and hypocone of M2 separated (ch. 132^{1-0}). Among the sister taxa, *Iranotherium* and *Ningxiatherium* are resolved basally. This result is consistent with Deng (2008) and Sun et al. (2022). *Sinotherium* and *Elasmotherium* constitute a branch (Node E) representing more derived taxa. Node E is supported by 14 equivocal synapomorphies: rostral end of nasal bones narrow (ch. 24^{1-0}), median nasal horn absent (ch. 27^{1-0}), frontal horn present (ch. 31^{0-1}), occipital crest forked (ch. 36^{1-2}), processus postglenoidalis of the squamosal dihedron in shape (ch. 42^{1-2}), foramen nervi hypoglossi of the basioccipital shift antero-externally (ch. 43^{0-1}), enamel foldings of cheek teeth are well developed (ch. 64^{1-2}), crochet of P2–4 is always simple (ch. 85^{1-0}), metaloph constriction of P2–4 absent (ch. 86^{1-0}), antecrochet of P2–3 usually present (ch. 90^{0-2}), protoloph of P2 not connected to the ectoloph (ch. 99^{0-1}), protocone and hypocone of P3–4 are separated (ch. 102^{3-2}), crista of P3 usually present (ch. 105^{3-2}), antecrochet of P4 is present (ch. 107^{0-3}). The members of *Elasmotherium* characterized by a very specialized huge frontal horn form a single lineage (Node F), which appear a relatively late in the elasmotheres. Node F is supported by 13 equivocal synapomorphies: anterior border of orbit above M3 (ch. 7^{2-1}), the radio of compared length of the premolars/molars rows is $<$ 42% (ch. 63^{1-2}), crown of cheek teeth is hypsodont (ch. 69^{2-3}), crochet of P2–4 always absent (ch. 84^{1-0}), postfossette of P2–4 has a posterior wall (ch. 89^{1-2}), antecrochet of P2–3 always present (ch. 90^{2-3}), P2 absent (ch. 93^{0-1}), crochet of upper molars always absent (ch. 111^{1-0}), paracone fold of M1–2 is absent (ch. 117^{0-1}), postfossette of M1 usually absent (ch. 127^{0-1}), external groove of lower cheek teeth developed (ch. 140^{2-0}), p2 always absent (ch. 153^{0-2}), hypolophid of lower molars almost sagittal (ch. 161^{1-2}).

Discussion

All evidence being considered, the new specimen from Tongxin (IVPP V23531) is different from all the known taxa of the tribe Elasmotheriini. Therefore, the new specimen is assigned to a new taxon, *Tongxinotherium latirhinum* gen. et sp. nov. (Fig. 4). It has a relatively larger size compared with the early elasmotheres *Bugtirhinus*, *Caementodon* and *Hispanotherium*. The rostral end of the nasal bone is very broad, rugose, and thick. The dorsal profile of the skull is straight; the 'U'-shaped nasal notch is located at the level of P3; the anterior margin of the orbit is situated at the level of M2. Teeth are subhypsodont, covered and filled by plentiful cement; enamel foldings are slightly developed; the protocone is expanded, with anterior and posterior constrictions. On the premolars, the posterior valley is closed; protocone and hypocone are connected; crochet, crista, and antecrochet are developed. On the molars, the paracone fold is developed; the ectoloph is curved. Buccal and lingual cingula are present on premolars but absent on molars (Fig. 5).

According to the morphological comparison and phylogenetic analysis, we summarize the general evolutionary trends of elasmotheres: (1) The skull shows a tendency for the longer head shape to become a comparatively short one. In order to adapt to the huge horn, one strategy is to move the position of the horn backward, another strategy is to shorten the skull. The early elasmotheres such as *Hispanotherium* and *Tongxinotherium* only have smaller nasal horns, and later nasal horns of *Parelasmotherium*, *Iranotherium* and *Ningxiatherium* gradually increase in size. *Sinotherium* has a nasofrontal horn and frontal horn. Finally, *Elasmotherium* evolved a huge frontal horn. (2) The nasal notch deepens by degrees, and the position of the anterior orbital tends to be more posterior on the skull. The posterior edge of the nasal notch of *Tongxinotherium latirhinum*, *Iranotherium morgani*, *Parelasmotherium linxiaense*, and *Ningxiatherium euryrhinus* is located at the level of P3, P2/P3, P4/M1 and P3/P4, respectively. Also, the anterior margin of the orbit of the species mentioned above is situated at the level of M2, M3, M3, and the level behind M3, respectively.

Kretzoi (1942) divided Elasmotheriidae into two subfamilies according to the position of the horn. One subfamily is Iranotheriinae with a nasal horn, and the other subfamily is Elasmotheriinae with a huge frontal horn. In the evolutionary sequence of elasmotheres, the primitive taxa have a small nasal horn, the more derived taxa have a long nasal horn, and the most derived elasmotheres have a huge frontal horn (Fig. 3). This process is

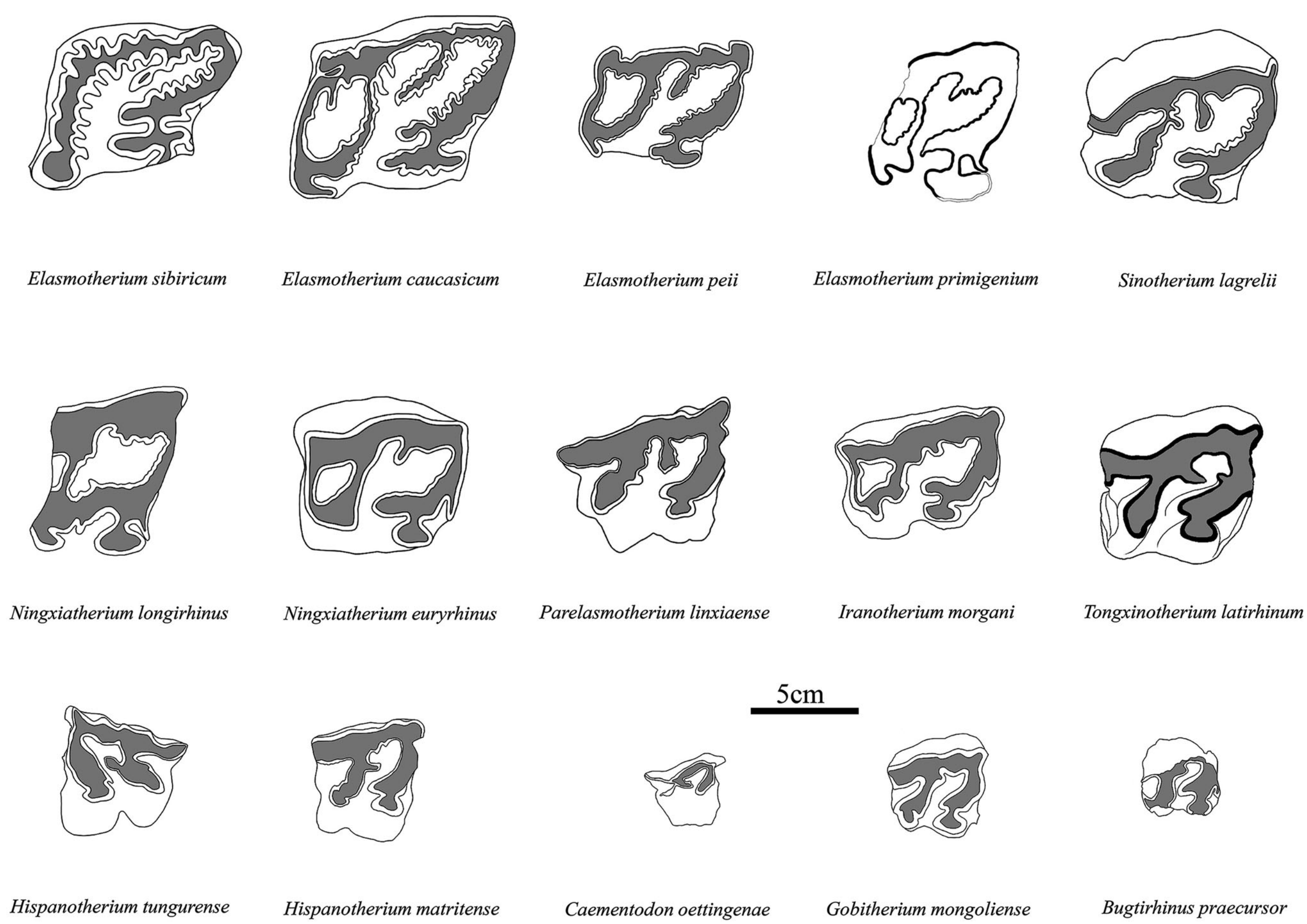

Figure 5. A series of M2 of elasmothere species from the early Miocene to the late Pleistocene.

accompanied by changes in other parts of the skull, such as the gradual ossification of the nasal septum, the gradual shortening of the skull, and the gradual forward movement of the cheek dentition. *Tongxinotherium latirhinum* is more derived than the early elasmotheres, and more primitive than *Iranotherium* and *Ningxiatherium*, bridging a morphological and stratigraphical gap between them. The discovery of new material improves the morphological characteristics of the early elasmotheres' horns and increases the diversity of the middle Miocene elasmotheres.

Conclusions

The new material described here from the middle Miocene of East Miaoerling (Tongxin County, Ningxia Province) is a dorsoventrally compressed skull with both cheek tooth rows (left and right P2–M3), lacking the occipital, and is morphologically distinct compared to any previously described species within the tribe Elasmotheriini. The skull is characterized by the broad and thick nasal bone, the 'U'-shaped nasal notch located at the level of P3, the anterior margin of the orbit situated at the level of M2, subhypsodont teeth covered and filled by plentiful cement, slightly developed enamel foldings, expanded protocone with anterior and posterior constrictions, the middle valley and posterior valley closed on the premolars, protoloph separated from the ectoloph on P2, and buccal and lingual cingula present on premolars, but absent on molars. Based on the aforementioned combination of features, we herein establish the new taxon *Tongxinotherium latirhinum* gen. et sp. nov.

According to the morphological comparison and phylogenetic analysis, *Tongxinotherium latirhinum* is more derived than the early elasmotheres, such as *Bugtirhinus*, *Caementodon* and *Hispanotherium*, and more primitive than the relatively large elasmotheres *Iranotherium* and *Ningxiatherium*. *Tongxinotherium latirhinum* is clearly nested within the clade of Elasmotheriini, and its origin and evolution in Eurasia are relatively well established. The discovery of new material increases the morphological variety of the early elasmotheres' horns, further enriches the fossil record of the middle Miocene elasmotheres, and provides new material for studying the diversity of elasmotheres.

Disclosure statement

No potential conflict of interest was reported by the author(s).

Acknowledgements

We thank Prof. Zhanxiang Qiu for his constructive suggestions and comments. We thank Yu Chen and Xiaocong Guo for their illustrations; Wei Gao for his photographs; Dan Su for her assistance in the repair of the fossil. We are grateful to the editors Zerina Johanson, Sue Greene, Jérémy Tissier, an anonymous reviewer, and especially Pierre-Olivier Antoine for their constructive comments and criticisms. We thank the Second Comprehensive Scientific Expedition on the Tibetan Plateau (2019QZKK0705). This research was supported by the Chinese Academy of Sciences (XDB26000000, XDA20070203, QYZDY-SSW-DQC022) and the National Natural Science Foundation of China (42172001).

Supplemental material

Supplemental material for this article can be accessed here: http://dx.doi.org/10.1080/14772019.2023.2236619.

ORCID

Danhui Sun http://orcid.org/0000-0001-8082-5595

References

Aguirre, E., & **Guerin, C.** (1974). Premiere decouverte d'un Iranotheriinae (Mammalia, Perissodactyla, Rhinocerotidae) en Afrique: *Kenyatherium bishopi* nov. gen. nov. sp. de la formation vallesienne (Miocene superior) de Nakali, Kenya. *Estudios geologicos*, *30*, 229–233.

Antoine, P.-O. (2002). Phylogénie et Évolution Des Elasmotheriina (Mammalia, Rhinocerotidae). *Mémoires du Muséum National d'Histoire Naturelle*, *188*, 1–359.

Antoine, P.-O. (2003). Middle Miocene elasmotheriine Rhinocerotidae from China and Mongolia: taxonomic revision and phylogenetic relationships. *Zoologica Scripta*, *32*, 95–118, https://doi.org/10.1046/j.1463-6409.2003.00106.x

Antoine, P.-O., **Alférez, F.**, & **Iñigo, C.** (2002). A new elasmotheriine (Mammalia, Rhinocerotidae) from the Early Miocene of Spain. *Comptes Rendus Palevol*, *1*, 19–26, https://doi.org/10.1016/S1631-0683(02)00005-2

Antoine, P.-O., & **Welcomme, J.-L.** (2000). A new rhinoceros from the Lower Miocene of the Bugti Hills, Baluchistan, Pakistan: the earliest elasmotheriine. *Palaeontology*, *43*, 795–816, https://doi.org/10.1111/1475-4983.00150

Antunes, M. T. 1979. *Hispanotherium* fauna in Iberian Middle Miocene; its importance and paleogeographical meaning; pp. 25–33 in Annales Geologiques Pays. Hellèn. VII International Congress on Mediterranean Neogene,

1979. Athens, 27 September–2 October 1978. Laboratoire de Géologie de L'Université.

Antunes, M., & **Ginsburg, L.** (1983). Les rhinocerotides du Miocene de Lisbonne-systematique, ecologie, paleobiogeographie, valeur stratigraphique. *Ciencias da Terra (UNL)*, *7*, 17–98.

Cerdeño, E. (1992). New remains of the rhinocerotid *Hispanotherium matritense* at La Retama site: Tagus Basin, Cuenca, Spain. *Geobios*, *25*, 671–679, https://doi.org/10.1016/0016-6995(92)80106-N

Cerdeño, E. (1996). Rhinocerotidae from the Middle Miocene of the Tung-gur Formation, Inner Mongolia (China). *American Museum Novitates*, *3184*, 1–43.

Cerdeño, E., & **Nieto, M.** (1995). Changes in Western European Rhinocerotidae related to climatic variations. *Palaeogeography, Palaeoclimatology, Palaeoecology*, *114*, 325–338, https://doi.org/10.1016/0031-0182(94)00085-M

Chen, G. (1977). A new genus of Iranotheriinae of Ningxia. *Vertebrata PalAsiatica*, *15*, 143–147.

Chen, G.-F. (1978). Fossil proboscideans from the Miocene of Zhongning-Tongxin area, Ningxia. *Vertebrata PalAsiatica*, *16*, 103–110, https://doi.org/10.19615/j.cnki.1000-3118.1978.02.005

Chow, M. (1958). New elasmotherine rhinoceroses from Shansi. *Vertebrata PalAsiatica*, *2*, 131–142.

Deng, T. (2001). New remains of *Parelasmotherium* (Perissodactyla, Rhinocerotidae) from the late Miocene in Dongxiang, Gansu, China. *Vertebrata PalAsiatica*, *39*, 306–311.

Deng, T. (2003). New material of *Hispanotherium matritense* (Rhinocerotidae, Perissodactyla) from Laogou of Hezheng County (Gansu, China), with special reference to the Chinese Middle Miocene elasmotheres. *Geobios*, *36*, 141–150, https://doi.org/10.1016/S0016-6995(03)00003-2

Deng, T. (2005). New cranial material of *Shansirhinus* (Rhinocerotidae, Perissodactyla) from the Lower Pliocene of the Linxia Basin in Gansu, China. *Geobios*, *38*, 301–313, https://doi.org/10.1016/j.geobios.2003.12.003

Deng, T. (2007). Skull of *Parelasmotherium* (Perissodactyla, Rhinocerotidae) from the upper Miocene in the Linxia Basin (Gansu, China). *Journal of Vertebrate Paleontology*, *27*, 467–475. https://doi.org/10.1671/0272-4634(2007)27[467:SOPPRF2.0.CO;2]

Deng, T. 2008. A new elasmothere (Perissodactyla, Rhinocerotidae) from the late Miocene of the Linxia Basin in Gansu, China. *Geobios*, *41*, 719–728. https://doi.org/10.1016/j.geobios.2008.01.006

Deng, T., & **Downs, W.** (2002). Evolution of Chinese Neogene Rhinocerotidae and its response to climatic variations. *Acta Geologica Sinica*, *76*, 139–145.

Deng, T., & **Wang, X.** (2004). New material of the Neogene rhinocerotids from the Qaidam Basin in Qinghai, China. *Vertebrata PalAsiatica*, *42*, 216–229.

Deng, T., **Wang, S.**, & **Hou, S.** (2013). A bizarre tandem-horned elasmothere rhino from the Late Miocene of northwestern China and origin of the true elasmothere. *Chinese Science Bulletin*, *58*, 1811–1817, https://doi.org/10.1007/s11434-012-5574-4

Dollo, L. 1885. Rhinocéros vivants et fossiles. *Revue des Questions Scientifiques*, *17*, 293–300.

Fischer, G. (1808). Notice d'un animal fossile de Sibérie inconnu aux naturalists. *Programme d'invitation à la séance publique de la Société Impériale des naturalistes de Moscou*, *4*, 19–20.

Geraads, D., **Lehmann, T.**, **Peppe, D. J.**, & **McNulty, K. P.** (2016). New Rhinocerotidae from the Kisingiri localities (lower Miocene of western Kenya). *Journal of Vertebrate Paleontology*, *36*, e1103247, https://doi.org/10.1080/02724634.2016.1103247

Geraads, D., **McCrossin, M.**, & **Benefit, B.** (2012). A new rhinoceros, *Victoriaceros kenyensis* gen. et sp. nov., and other Perissodactyla from the Middle Miocene of Maboko, Kenya. *Journal of Mammalian Evolution*, *19*, 57–75, https://doi.org/10.1007/s10914-011-9183-9

Geraads, D., & **Zouhri, S.** (2021). A new late Miocene elasmotheriine rhinoceros from Morocco. *Acta Palaeontologica Polonica*, *66*, 753–765, https://doi.org/10.4202/app.00904.2021

Ginsburg, L., **Maubert, F.**, & **Telles Antunes, M.** (1987). Découverte d'*Hispanotherium* et de gaindatherium (Rhinocerotidae, Mammalia) dans 1e Miocène de France. *Bulletin du Muséum Nationale d'Histoire Naturelle, Section C*, *9*, 303–311.

Guan, J. (1988). The Miocene strata and mammals from Tongxin, Ningxia and Guanghe, Gansu. *Memoirs of Beijing Natural History Museum*, *42*, 1–21.

Guan, J. (1993). Primitive elasmotherines from the middle Miocene, Ningxia (northwestern China). *Memoirs of Beijing Natural History Museum*, *53*, 200–207.

Guan, J., & **Van der Made, J.** (1993). Fossil Suidae from Dingjiaergou near Tongxin, China. *Memoirs of the Beijing Natural History Museum*, *53*, 150–199.

Guérin, C. (1980). Les rhinocéros (Mammalia, Perissodactyla) du Miocène terminal au Pléistocène supérieur en Europe occidentale. Comparaison avec les espèces actuelles (fascicule 1). *Travaux et Documents des Laboratoires de Géologie de Lyon*, *79*, 1–1184.

Guérin, C., & **Pickford, M.** (2003). *Ougandatherium napakense* nov. gen. nov. sp., le plus ancien Rhinocerotidae Iranotheriinae d'Afrique. *Annales de Paléontologie*, *89*, 1–35, https://doi.org/10.1016/S0753-3969(03)00004-1

Handa, N. (2016). *Fossil Rhinoceroses from the Late Miocene of Kenya – Miocene faunal changes of the Rhinocerotidae (Mammalia, Perissodactyla) in SubSaharan East Africa* [Unpublished PhD thesis]. Kagoshima University.

Handa, N., **Nakatsukasa, M.**, **Kunimatsu, Y.**, & **Nakaya, H.** (2017). A new Elasmotheriini (Perissodactyla, Rhinocerotidae) from the upper Miocene of Samburu Hills and Nakali, northern Kenya. *Geobios*, *50*, 197–209, https://doi.org/10.1016/j.geobios.2017.04.002

Harrison, T., **Delson, E.**, & **Jian, G.** (1991). A new species of *Pliopithecus* from the middle Miocene of China and its implications for early catarrhine zoogeography. *Journal of Human Evolution*, *21*, 329–361. https://doi.org/10.1016/0047-2484(91)90112-9

Heissig, K. 1972. Paläontologische und geologische Untersuchungen im Tertiär von Pakistan. 5. Rhinocerotidae (Mammalia) aus den unteren und mittleren Siwalik-Schichten. *Abhandlungen der Bayerischen Akademie der Wissenschaften, Mathematisch-Naturwissenschaftliche Klasse, München* **152**: 1–112.

Heissig, K. (1996). The stratigraphical range of fossil rhinoceroses in the Late Neogene of Europe and the Eastern Mediterranean. In R. L. Bernor, V. Fahlbusch, H.-W. Mittmann (Eds.), *The evolution of western Eurasian Neogene mammal faunas* (pp. 339–347). Columbia University Press.

Heissig, K. (1999). Family Rhinocerotidae. In G. E. Rössner, & K. Heissig (Eds.), *The Miocene land mammals of Europe* (pp. 175–188). Verlag Dr. F. Pfeil.

Hernández-Pacheco, F., & **Crusafont, M.** (1960). Primera caracterización paleontológica del Terciario de Extremadura. *Boletín de la Real Sociedad Española de Historia Natural (Geologia)*, *58*, 275–282.

Huang, W., & **Yan, D.** (1983). New material of Elasmotherini [sic] from Shennongjia, Hubei. *Vertebrata PalAsiatica*, *21*, 223–229, https://doi.org/10.19615/j.cnki.1000-3118.1983.03.006

Iñigo, C., & **Cerdeño, E.** (1997). The *Hispanotherium matritense* (Rhinocerotidae) from Córcoles (Guadalajara, Spain): its contribution to the systematics of the Miocene Iranotheriina. *Geobios*, *30*, 243–266, https://doi.org/10.1016/S0016-6995(97)80232-X

Jiangzuo, Q., **Li, C.**, **Wang, S.**, & **Sun, D.** (2018). *Amphicyon zhanxiangi* sp. nov., a new amphicyonid (Mammalia, Carnivora) from northern China. *Journal of Vertebrate Paleontology*, *38*, e1539857, https://doi.org/10.1080/02724634.2018.1539857

Jiangzuo, Q., **Wang, S.**, **Li, C.**, **Sun, D.**, & **Zhang, X.** (2021). New material of *Gobicyon* (Carnivora, Amphicyonidae, Haplocyoninae) from Northern China and a review of Aktaucyonini evolution. *Papers in Palaeontology*, *7*, 307–327, https://doi.org/10.1002/spp2.1283

Killgus, H. (1923). Unterpliozäne Säuger aus China. *Paläontologische Zeitschrift*, *5*, 251–257.

Kosintsev, P., **Mitchell, K. J.**, **Devièse, T.**, **van der Plicht, J.**, **Kuitems, M.**, **Petrova, E.**, **Tikhonov, A.**, **Higham, T.**, **Comeskey, D.**, **Turney, C.**, **Cooper, A.**, **van Kolfschoten, T.**, **Stuart, A. J.**, & **Lister, A. M.** (2019). Evolution and extinction of the giant rhinoceros *Elasmotherium sibiricum* sheds light on late Quaternary megafaunal extinctions. *Nature Ecology & Evolution*, *3*, 31–38, https://doi.org/10.1038/s41559-018-0722-0

Kretzoi, M. (1942). Bemerkungen zum system der nachmiozänen Nashorn-Gattungen. *Földtani Közlöny*, *72*, 309–318.

Mecquenem, R. (1908). *Contribution à l'étude Du Gisement des Vertébrés de Maragha et de Ses Environs*. *E. Leroux, Annales d'Histoire Naturelle*.

Nakaya, H., **Pickford, M.**, **Yasui, K.**, & **Nakano, Y.** (1987). Additional large mammalian fauna from the Namurungule Formation, Samburu Hills, northern Kenya. *African Study Monographs*, suppl. issue 5, 79–129.

Owen, R. 1845. *A history of British fossil mammals and birds*. J. van Voorst.

Owen, R. 1848. *On the archetype and homologies of the vertebrate skeleton*. J. Van Voorst.

Qiu, Z., & **Xie, J.** (1998). Notes on *Parelasmotherium* and *Hipparion* fossils from Wangji, Dongxiang, Gansu. *Vertebrata PalAsiatica*, *36*, 13–23.

Qiu Z., **Ye J.**, & **Huo F.** (1988). Description of a Kubanochoerus skull from Tongxin, Ningxia. *Vertebrata PalAsiatica*, *26*, 1–19, https://doi.org/10.19615/j.cnki.1000-3118.1988.01.001

Ringström, T. (1923). *Sinotherium lagrelii*, a new fossil rhinocerotid from Shansi. *Bulletin of the Geological Survey of China*, *5*, 91–93.

Ringström, T. (1924). Nashorner der hipparion-fauna nord-chinas. *Geological Survey of China, Series C*, *11*, 1–156.

Sanisidro, O., **Alberdi, M. T.**, & **Morales, J.** (2012). The first complete skull of *Hispanotherium matritense* (Prado) (Perissodactyla, Rhinocerotidae) from the middle Miocene of the Iberian Peninsula. *Journal of Vertebrate Paleontology*, *32*, 446–455, https://doi.org/10.1080/02724634.2012.639420

Schvyreva, A. K. (2015). On the importance of the representatives of the genus *Elasmotherium* (Rhinocerotidae, Mammalia) in the biochronology of the Pleistocene of Eastern Europe. *Quaternary International*, *379*, 128–134, http://dx.doi.org/10.1016/j.quaint.2015.03.052

Sun, D., **Deng, T.**, & **Jiangzuo, Q.** (2022). The most primitive *Elasmotherium* (Perissodactyla, Rhinocerotidae) from the Late Miocene of northern China. *Historical Biology*, *34*, 201–211. https://doi.org/10.1080/08912963.2021.1907368

Sun, B.-Y., **Wang, X.-X.**, **Ji, M.-X.**, **Pang, L.-B.**, **Shi, Q.-Q.**, **Hou, S.-K.**, **Sun, D.-H.**, & **Wang, S.-Q.** (2018). Miocene mammalian faunas from Wushan, China and their evolutionary, biochronological, and biogeographic significances. *Palaeoworld*, *27*, 258–270, https://doi.org/10.1016/j.palwor.2017.08.001

Swofford, D. L. (2002). *PAUP*. Phylogenetic analysis using parsimony (*and other methods)*, Version 4. Sinauer Associates.

Tong, H., & **Moigne, A.-M.** (2000). Quaternary Rhinoceros of China. *Acta Anthropologica Sinica*, *19*, 257–263.

Wang, S., **Deng, T.**, **Tang, T.**, **Xie, G.**, **Zhang, Y.**, & **Wang, D.** (2015). Evolution of *Protanancus* (Proboscidea, Mammalia) in East Asia. *Journal of Vertebrate Paleontology*, *35*, e881830, https://doi.org/10.1080/02724634.2014.881830

Wang, S., **Zong, L.**, **Yang, Q.**, **Sun, B.**, **Li, Y.**, **Shi, Q.**, **Yang, X.**, **Ye, J.**, & **Wu, W.** (2016). Biostratigraphic subdividing of the Neogene Dingjia'ergou mammalian fauna, Tongxin County, Ningxia Province, and its background for the uplift of the Tibetan Plateau. *Quaternary Sciences*, *36*, 789–809.

Wang, S.-Q., **Deng, T.**, **Ye, J.**, **He, W.**, & **Chen, S.-Q.** (2017). Morphological and ecological diversity of Amebelodontidae (Proboscidea, Mammalia) revealed by a Miocene fossil accumulation of an upper-tuskless proboscidean. *Journal of Systematic Palaeontology*, *15*, 601–615, https://doi.org/10.1080/14772019.2016.1208687

Wang, X., **White, S. C.**, & **Guan, J.** (2020). A new genus and species of sabretooth, *Oriensmilus liupanensis* (Barbourofelinae, Nimravidae, Carnivora), from the middle Miocene of China suggests barbourofelines are nimravids, not felids. *Journal of Systematic Palaeontology*, *18*, 783–803. https://doi.org/10.1080/14772019.2019.1691066

Wang, X., **Xie, G.**, & **Dong, W.** (2009). A new species of crown-antlered deer *Stephanocemas* (Artiodactyla, Cervidae) from the middle Miocene of Qaidam Basin, northern Tibetan Plateau, China, and a preliminary evaluation of its phylogeny. *Zoological Journal of the Linnean Society*, *156*, 680–695, https://doi.org/10.1111/j.1096-3642.2008.00491.x

Werdelin, L., & **Solounias, N.** (1991). The Hyaenidae: taxonomy, systematics and evolution. *Fossils and Strata*, *30*, 1–104.

Wu, W., **Ye, J.**, & **Zhu, B.** (1991). On *Alloptox* (Lagomorpha, Ochoronidae) from the middle Miocene of Tongxin, Ningxia Hui Autonomous Region, China. *Gujizhui Dongwu Xuebao*, *29*, 204–229.

Xiong, W. (2022). New species of *Percrocuta* (Carnivora, Hyaenidae) from the early middle Miocene of Tongxin, China. *Historical Biology*, 1–22, https://doi.org/10.1080/08912963.2022.2067757

Yan D. (1979). Einige der Fossilen Miozänen Säugetiere der Kreis von Fangxian in Der Provinz Hupei. *Vertebrata Palasiatica*, *17*, 189–199, https://doi.org/10.19615/j.cnki.1000-3118.1979.03.002

Ye J., & **Jia H.** (1986). *Platybelodon* (Proboscidea, Mammalia) from the Middle Miocene of Tongxin, Ningxia. *Vertebrata PalAsiatica*, *24*, 139–151, https://doi.org/10.19615/j.cnki.1000-3118.1986.02.005

Ye, J., **Qiu, Z.**, & **Zhang, G.** (1992). *Bunolistriodon intermedius* (Suidae, Artiodactyla) from Tongxin, Ningxia. *Vertebrata PalAsiatica*, *30*, 135–145.

Zhai, R. J. (1978). A primitive elasmothere from the Miocene of Lintung. Shensi. *Professional Papers of Stratigraphy and Palaeontology*, *7*, 122–126.

Associate Editor: Jérémy Tissier